EJN fens European Journal of Neuroscience

European Journal of Neuroscience, Vol. 34, pp. 605–614, 2011 doi:10.1111/j.1460-9568.2011.07778.x

NEUROSYSTEMS

Bifrontal transcranial direct current stimulation modulates tinnitus intensity and tinnitus-distress-related brain activity

Sven Vanneste and Dirk De Ridder
Brai2n, TRI and Department of Neurosurgery, University Hospital Antwerp, Wilrijkstraat 10, 2650 Edegem, Belgium

Keywords: electroencephalography, functional connectivity, gamma, human, phase synchronization, standardized low-resolution brain electromagnetic tomography

Abstract

Bifrontal transcranial direct current stimulation (tDCS), with the anodal electrode overlying the right and the cathodal electrode overlying the left dorsolateral prefrontal cortex, has been shown to suppress tinnitus significantly in 30% of patients. The source localized resting-state electrical activity is recorded before and after bifrontal tDCS in patients who respond to tDCS to unravel the mechanism by which tDCS suppresses tinnitus. The present electroencephalography study ($N = 12$) provides support for the ability of bifrontal tDCS to suppress tinnitus intensity and tinnitus-related distress by modulation of the pregenual anterior cingulate cortex, parahippocampal area and right primary auditory cortex in resting-state spontaneous brain activity. These findings provide direct support for tDCS having an impact not only directly on the underlying dorsolateral prefrontal cortex but also indirectly on functionally connected brain areas relevant for tinnitus distress and tinnitus intensity, respectively.

Introduction

Tinnitus is a common and disturbing symptom, characterized by the perception of sound or noise in the absence of an external auditory stimulus. Ten to fifteen percent of the Western population perceives tinnitus continuously (Axelsson & Ringdahl, 1989). This auditory phantom percept is often associated with symptoms such as anxiety (Langguth *et al.*, 2007), depression (Langguth *et al.*, 2007), sleep disturbances (Cronlein *et al.*, 2007) and distress (Scott & Lindberg, 2000).

Recently, transcranial direct current stimulation (tDCS) has been reintroduced as a non-invasive procedure of cortical stimulation (Nitsche & Paulus, 2000; Nitsche *et al.*, 2001; Vanneste & De Ridder, 2011). When tDCS is applied in humans, a relatively weak constant direct current is passed through the cerebral cortex via scalp electrodes (Nitsche & Paulus, 2000). Depending on the polarity of the stimulation, tDCS can increase or decrease cortical excitability in the brain regions to which it is applied (Nitsche & Paulus, 2000). Currently, tDCS is usually applied through two surface electrodes, one serving as the anode and the other as the cathode. Some of the applied current is shunted through scalp tissue and only a part of the applied current passes through the brain (Dymond *et al.*, 1975). Anodal tDCS typically has an excitatory effect on the underlying cerebral cortex by depolarizing neurons, whereas the opposite occurs under the cathode due to induced hyperpolarization (Nitsche & Paulus, 2001; Nitsche *et al.*, 2003). This effect of tDCS typically outlasts the stimulation by an hour or longer after a single treatment session of sufficiently long stimulation duration (Nitsche & Paulus, 2000, 2001).

Several tDCS studies targeting the dorsolateral prefrontal cortex (DLPFC) demonstrated clinically beneficial results in treating major depression (Fregni *et al.*, 2006a), as well as reducing impulsiveness (Beeli *et al.*, 2008) and modulating the emotional response to pain-related pictures (Boggio *et al.*, 2009). In a recent study (Fregni *et al.*, 2006b), it was demonstrated that not only auditory cortex tDCS can modulate tinnitus perception but also bifrontal tDCS, placing the anodal electrode on the scalp overlying the right DLPFC and the cathodal electrode overlying the left DLPFC (Vanneste *et al.*, 2010b). However, in only 30% of patients does it exert a tinnitus-suppressing effect (Vanneste *et al.*, 2010b).

Although the clinical and functional changes induced by tDCS have been pursued, little is known about the underlying neurophysiological mechanisms. Such knowledge could lead to a better understanding of the working mechanism of tDCS as well as of the neurobiology of different pathologies in general and tinnitus in particular.

The effect of bifrontal tDCS on tinnitus intensity might be mediated via the DLPFC's inhibitory modulation of the auditory cortex (Knight *et al.*, 1989), which is involved in tinnitus intensity coding (van der Loo *et al.*, 2009), whereas tinnitus-related distress might be more directly suppressed via its local activity analogous to what has been observed in depression (Fregni *et al.*, 2006a). However, if tDCS and transcranial magnetic stimulation share some commonality in their working mechanism, an alternative hypothetical explanation for the observed effect might be related to a modulation of neural activity in the rostral or pregenual anterior cingulate cortex (prACC), which determines whether transcranial magnetic stimulation on the auditory cortex results in successful tinnitus distress suppression (Plewnia *et al.*, 2006).

Correspondence: S. Vanneste, as above.
E-mail: sven.vanneste@ua.ac.be

Received 27 December 2010, revised 21 May 2011, accepted 25 May 2011

In order to understand how frontal tDCS modulates an auditory phantom percept, this present study probes the neurophysiological differences before and after tDCS in a group of patients with tinnitus who are known to respond in a single-blinded placebo-controlled way to bifrontal tDCS. We used electroencephalography (EEG) recordings to localize the cortical sources of resting-state electrical brain activity associated with a clinical tinnitus reduction induced by bifrontal tDCS.

Materials and methods

Patients

Twelve subjects suffering from chronic tinnitus participated in the study (nine males, three females). The mean age was 50.45 years (range 41–56 years) and the mean tinnitus duration was 4.75 years (SD 1.02 years). Subjects were included if they had already responded to bifrontal tDCS a minimum of 4 months before the study started and had suppression of a minimum of 25% on both tinnitus perception ('How loud is your tinnitus?') and tinnitus distress ('How distressful is your tinnitus?'), and had no placebo response during the sham stimulation. These patients were selected from a database of 100 patients of whom 29 patients were responders to tDCS. Twelve patients were willing to collaborate in this study.

Of the 12 patients, three reported dominant left, seven bilaterally equal and two dominant right lateralized tinnitus. Seven subjects reported narrow-band noise tinnitus and five reported pure-tone tinnitus.

The study protocol has been approved by the Antwerp University Hospital IRB ('Comité voor medische ethiek').

Transcranial direct current stimulation

Direct current was transmitted by a saline-soaked pair of surface sponges (35 cm^2) and delivered by a specially developed, battery-driven, constant current stimulator with a maximum output of 10 mA (Neuroconn; http://www.neuroconn.de/). For each patient receiving tDCS the negative electrode (cathode) was placed over the left DLPFC and the positive electrode (anode) was placed on the right DLPFC as determined by the International 10/20 Electroencephalogram System corresponding to F3 and F4, respectively. A constant current of 1.5 mA intensity was applied for 20 min. For sham tDCS, placement of the electrodes was identical to real tDCS. Direct current was first switched on in a ramp-up fashion over 5 s. Current intensity (ramp down) was gradually reduced (over 5 s) as soon as the direct current reached a current flow of 1.5 mA. Hence, sham tDCS only lasted 10 s. The rationale behind this sham procedure was to mimic the transient skin sensation at the beginning of real tDCS without producing any conditioning effects on the brain. The order of the sham and real tDCS was randomized over the different patients. There was 1 week between the two stimulations. Only patients were blinded to the stimulation design (i.e. single blinded).

A visual analogue scale for tinnitus perception ('How loud is your tinnitus?' 0, no tinnitus and 10, as loud as imaginable) and tinnitus distress ('How stressful is your tinnitus?' 0, no distress and 10, suicidal distress) was used before (pre) and directly after (post) tDCS stimulation.

For comparing pre- and post-tDCS results on tinnitus perception and tinnitus distress, a Wilcoxon signed rank test (one-tailed) was performed as our results were not normally distributed due to the small sample size. A similar analysis was performed comparing pre-tDCS results of the current study with the results obtained in the same patients 4 months previously as well as post-tDCS results for both tinnitus intensity and tinnitus distress. In addition, Pearson correlations were also calculated between the amount of suppression (pre-tDCS – post-tDCS) in the current study and the results obtained 4 months previously.

Electroencephalography recording

The EEG recordings (Mitsar-201, NovaTech, http://www.novate-cheeg.com/) were obtained in a fully lighted room with each participant sitting upright on a small but comfortable chair. The actual recording lasted approximately 5 min. The EEG was sampled with 19 electrodes (Fp1, Fp2, F7, F3, Fz, F4, F8, T7, C3, Cz, C4, T8, P7, P3, Pz, P4, P8, O1 and O2) in the standard 10/20 international placement, referenced to linked ears and impedances were checked to remain below 5 kΩ. Data were collected with the eyes closed (sampling rate, 1024 Hz; band-passed, 0.15–200 Hz). Data were resampled to 128 Hz, band-pass filtered (fast Fourier transform filter) to 2–44 Hz and subsequently transposed into EUREKA! Software (Congedo, 2002), plotted and carefully inspected for manual artifact rejection (i.e. episodic artifacts including eye blinks, eye movements, teeth clenching, body movement or electrocardiography artifact). In addition, an independent component analysis (ICA) was conducted to further verify whether all artifacts were excluded. To investigate the effect of possible ICA component rejection, we compared the power spectra in two approaches: (i) after visual artifact rejection only (before ICA) and (ii) after additional ICA component rejection (after ICA). To test for significant differences between the two approaches we performed a repeated-measure ANOVA, considering the mean band power as the within-subject variables. Average Fourier cross-spectral matrices were computed for the bands delta (2–3.5 Hz), theta (4–7.5 Hz), alpha1 (8–10 Hz), alpha2 (10–12 Hz), beta1 (13–18 Hz), beta2 (18.5–21 Hz), beta3 (21.5–30 Hz) and gamma (30.5–44 Hz). We then computed the discrete frequencies between 2 and 44 Hz. The EEG was recorded before the real or sham stimulation and immediately (i.e. 1 min) after real or sham tDCS with associated reporting of the tinnitus perception and tinnitus distress.

Source localization

Standardized low-resolution brain electromagnetic tomography (sLORETA) was used to estimate the intracerebral electrical sources that generated the scalp-recorded activity in each of the eight frequency bands (Pascual-Marqui, 2002). sLORETA computes the electric neuronal activity as current density (A/m^2) without assuming a predefined number of active sources. The sLORETA solution space consists of 6239 voxels (voxel size 5 × 5 × 5 mm) and is restricted to the cortical gray matter and hippocampi, as defined by the digitized Montreal Neurological Institute 152 template (Fuchs *et al.*, 2002). Scalp electrode coordinates on the Montreal Neurological Institute brain are derived from the international system (Jurcak *et al.*, 2007). The tomography of sLORETA has received considerable validation from studies combining LORETA with other more established localization methods, such as functional magnetic resonance imaging (Vitacco *et al.*, 2002; Mulert *et al.*, 2004), structural magnetic resonance imaging (Worrell *et al.*, 2000) and positron emission tomography (Dierks *et al.*, 2000; Pizzagalli *et al.*, 2004; Zumsteg *et al.*, 2005). Further sLORETA validation has been based on accepting as the ground truth the localization findings obtained from invasive, implanted depth electrodes, for which there are several studies in epilepsy (Zumsteg *et al.*, 2006a,c) and cognitive event-related potentials (Volpe *et al.*, 2007). It is worth emphasizing that deep structures such as the anterior cingulate cortex (Pizzagalli *et al.*,

2001) and mesial temporal lobes (Zumsteg *et al.*, 2006b) can also be correctly localized with these methods.

Connectivity

Brain connectivity can refer to a pattern of anatomical links ('anatomical connectivity'), statistical dependencies ('functional connectivity') or causal interactions ('effective connectivity') between distinct units within a nervous system (Honey *et al.*, 2007). The present research focuses on functional connectivity, which captures deviations from statistical independence between distributed and often spatially remote neuronal units. Statistical dependence may be estimated by measuring the correlation or covariance, spectral coherence or phase-locking (Sporns & Kotter, 2004; Sporns *et al.*, 2004; Friston, 2005).

Coherence and phase synchronization between time series corresponding to different spatial locations are usually interpreted as indicators of the 'connectivity'. However, any measure of dependence is highly contaminated with an instantaneous, non-physiological contribution due to volume conduction (Pascual-Marqui, 2007b). However, Pascual-Marqui (2007a) introduced a new technique (i.e. Hermitian covariance matrices) that removes this confounding factor. As such, this measure of dependence can be applied to any number of brain areas jointly, i.e. distributed cortical networks, the activity of which can be estimated with sLORETA. Measures of linear dependence (coherence) between the multivariate time series are defined. The measures are expressed as the sum of lagged dependence and instantaneous dependence. The measures are non-negative, and take the value zero only when there is independence and are defined in the frequency domain: delta (2–3.5 Hz), theta (4–7.5 Hz), alpha1 (8–10 Hz), alpha2 (10–12 Hz), beta1 (13–18 Hz), beta2 (18.5–21 Hz), beta3 (21.5–30 Hz) and gamma (30.5–45 Hz). Based on this principle, the lagged linear connectivity was calculated. The regions of interest were for the DLPFC [Brodmann Area (BA) 9 and BA46)] (Vanneste *et al.*, 2010b), prACC (left and right BA24, and left and right BA32) (Schlee *et al.*, 2009), left and right parahippocampus (PHC) (BA27 and BA29) (Vanneste *et al.*, 2010a, 2011) and right primary auditory cortex (A1) (Weisz *et al.*, 2007). These regions of interest were defined based on previous literature (Weisz *et al.*, 2007; Schlee *et al.*, 2009; Vanneste *et al.*, 2010a,c, 2011) as well as on the source localized EEGs.

Source analysis

In order to identify potential differences in brain electrical activity between conditions, sLORETA was then used to perform voxel-by-voxel between-condition comparisons of the current density distribution. Non-parametric statistical analyses of functional sLORETA images (statistical non-parametric mapping) were performed for each contrast employing a *t*-statistic for paired groups and corrected for multiple comparisons ($P < 0.05$). As explained by Nichols & Holmes (2002), the statistical non-parametric mapping methodology does not require any assumption of Gaussianity and corrects for all multiple comparisons. We performed one voxel-by-voxel test (comprising 6239 voxels each) for the different frequency bands.

Region of interest

Furthermore, the log-transformed electric current density was averaged across all voxels belonging to the region of interest, for DLPFC (BA9 and BA46), respectively, left and right separately for the delta (2–3.5 Hz), theta (4–7.5 Hz), alpha1 (8–10 Hz), alpha2 (10–12 Hz), beta1 (13–18 Hz), beta2 (18.5–21 Hz), beta3 (21.5–30 Hz) and gamma (30.5–45 Hz) frequency band.

For comparing pre- and post-tDCS log-transformed current densities, a Wilcoxon signed rank test was performed as our results were not normally distributed due to the small sample size.

The log-transformed electric current density was also averaged across all voxels belonging to the region of interest, for left and right DLPFC (BA9 and BA46) (Vanneste *et al.*, 2010b), prACC (left and right BA24, and left and right BA32) (Schlee *et al.*, 2009), left and right PHC (BA27 and BA29) (Vanneste *et al.*, 2010a, 2011) and the right A1 (Weisz *et al.*, 2007) separately for all discrete frequencies between 2 and 44 Hz.

Pearson autocorrelations were calculated for, respectively, the left and right DLPFC before and after tDCS. Further Pearson cross-correlations were calculated between the right DLPFC and, respectively, the prACC, left and right PHC, and right A1.

Results

Transcranial direct current stimulation results

A comparison was made between pre-sham and pre-real tDCS for, respectively, tinnitus perception [$Z(12) = -0.81$, $P = 0.42$; pre-real tDCS, $M = 6.83$, SD 1.52 vs. pre-sham tDCS, $M = 7.17$, SD 1.19] and tinnitus distress [$Z(12) = -1.13$, $P = 0.26$; pre-real tDCS, $M = 7.29$, SD 1.17 vs. pre-sham tDCS, $M = 7.54$, SD 0.98] indicating no significant differences. As pre-sham and pre-real tDCS do not differ, we combined them into one baseline score for, respectively, tinnitus perception and tinnitus distress.

The analysis indicated a significant effect for tinnitus perception [$Z(12) = -3.09$, $P < 0.01$] and tinnitus distress [$Z(12) = -3.07$, $P < 0.01$] (see Fig. 1). Comparing baseline with post-real tDCS, an improvement was demonstrated for tinnitus perception of 41.67% and tinnitus distress of 43.20%. A comparison between baseline and post-sham tDCS yielded no significant effect for both tinnitus perception [$Z(12) = -0.38$, $P = 0.56$] and tinnitus distress [$Z(12) = -0.71$, $P = 0.56$], whereas a comparison between post-real and post-sham tDCS yielded a significant effect for both tinnitus perception [$Z(12) = -3.10$, $P < 0.01$] and tinnitus distress [$Z(12) = -2.81$, $P < 0.01$]. All patients showed a reduction of a minimum of 25% on both tinnitus perception and tinnitus distress when comparing post-real tDCS with post-sham stimulation. The effect of the real tDCS

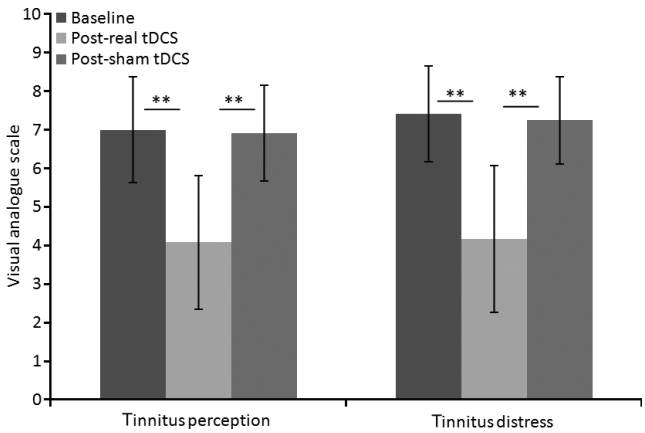

FIG. 1. Baseline, post-real tDCS and post-sham tDCS visual analogue scale for tinnitus perception and tinnitus distress (**$P < 0.01$).

remained for between a minimum of 18 h and a maximum of 62 h, with a mean duration of 24 h.

The patients' baseline scores for tinnitus perception (M = 7.00, SD 1.34) and tinnitus distress (M = 7.42, SD 1.24) did not differ in a significant way in comparison to the baseline scores 4 months previously for, respectively, tinnitus perception (M = 6.86, SD 1.21) and tinnitus distress (M = 7.33, SD 1.61) [$Z(12) = -0.45$, $P = 0.65$ and $Z(12) = -0.27$, $P = 0.78$]. No significant differences were obtained post-real tDCS between tinnitus perception (M = 4.08, SD 1.73) and tinnitus distress (M = 14.17, SD 1.91) in comparison to their post-real tDCS scores 4 months previously for perception (M = 433, SD 1.50) and tinnitus distress (M = 4.50, SD 1.68), respectively [$Z(12) = -1.34$, $P = 0.18$ and $Z(12) = -1.61$, $P = 0.11$]. In addition, a correlation showed that the amount of suppression for tinnitus perception ($r = 0.78$, $P < 0.01$) and tinnitus distress ($r = 0.67$, $P < 0.05$) in this study strongly correlated with the amount of suppression obtained 4 months previously.

Pre- vs. post-real transcranial direct current stimulation source analysis

Source analysis revealed a significant increase of alpha 1 activity after tDCS in the prACC in comparison to pre-tDCS (see Fig. 2). Significantly decreased activity was also found for beta3 and gamma in the right A1 and the inferior primary somatosensory cortex post-tDCS in comparison to pre-tDCS (see Fig. 2). Table 1 shows the significant voxels, respectively, for alpha1, beta3 and gamma frequency bands when comparing post-tDCS minus pre-tDCS. No significant effects were obtained for delta, theta, alpha2, beta1 and beta2.

Region of interest analysis: dorsolateral prefrontal cortex

A region of interest analysis revealed a significant decrease in current density for the left DLPFC after tDCS in comparison to pre-tDCS [$Z(12) = -2.04$, $P < 0.05$ for BA9 and $Z(12) = -2.22$, $P < 0.05$ for BA46] (see Fig. 3). In contrast, a region of interest analysis revealed a significant gamma increase in current density for the right DLPFC after tDCS in comparison to pre-tDCS [$Z(12) = 1.91$, $P = 0.05$ for BA9 and $Z(12) = 2.04$, $P < 0.05$ for BA46] (see Fig. 3). No significant differences were found for the other frequency bands, namely delta, theta, alpha1, alpha2, beta1, beta2 and beta3.

Functional connectivity

For the theta frequency band, increased lagged phase synchronization (functional connectivity) was found between the right DLPFC and, respectively, the left and right PHC and the right A1 when comparing post-real tDCS with pre-real tDCS (see Fig. 4A). Increased theta

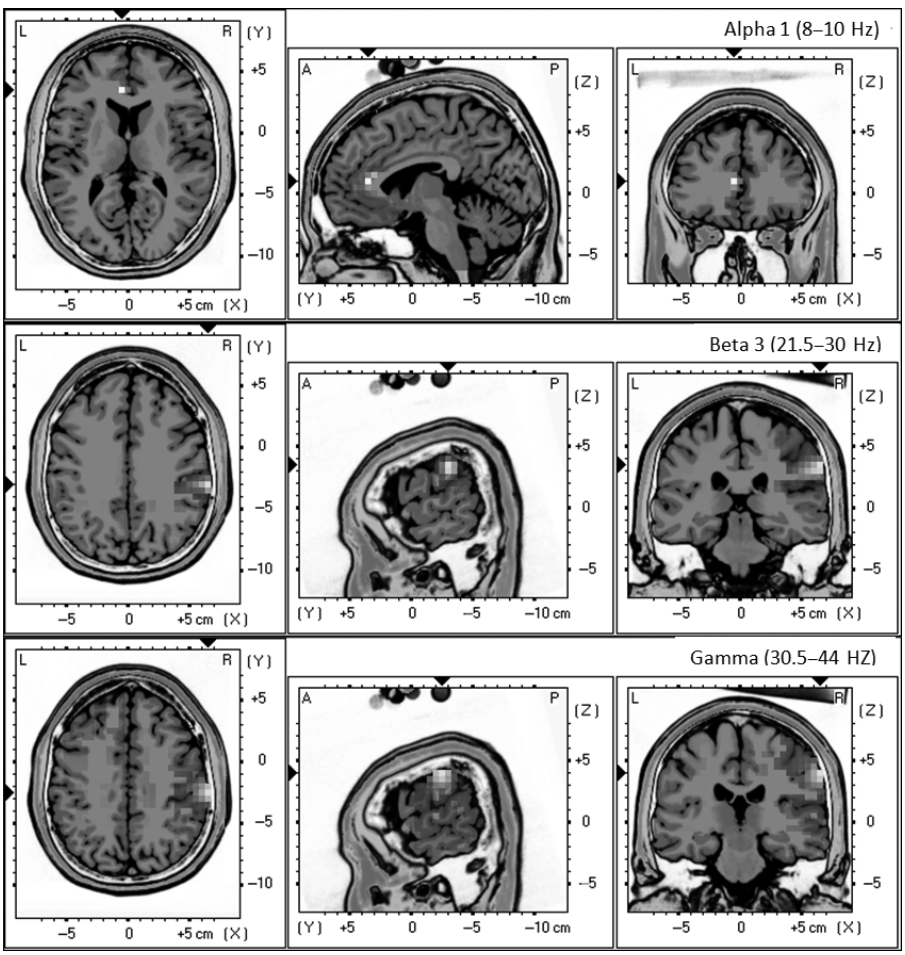

FIG. 2. Results for sLORETA analysis indicating significant increased synchronized activity in the prACC for the alpha 1 frequency band (8–10 Hz; top panel), and decreased synchronized activity in the A1 for the beta3 (21.5–30 Hz; middle panel) and gamma (30.5–44 Hz; bottom panel) frequency bands when comparing pre-real and post-real tDCS.

TABLE 1. Significant voxels and Montreal Neurological Institute coordinates for, respectively, alpha1, beta3 and gamma frequency bands when comparing pre-real and post-real tDCS

	X	Y	Z	Voxel value	Brodmann area	Name
Alpha1	−5	35	10	1.97	24	prACC
	−5	30	15	1.95	24	prACC
	−5	35	5	1.93	24	prACC
	−5	35	15	1.92	24	prACC
	0	30	15	1.92	24	prACC
	−5	25	15	1.92	24	prACC
	0	35	10	1.91	24	prACC
Beta3	65	−30	35	−2.35	40	Right A1
	65	−30	30	−2.34	40	Right A1
	60	−30	30	−2.34	40	Right A1
	60	−30	35	−2.35	40	Right A1
	55	−30	30	−2.33	40	Right A1
	65	−35	30	−2.32	40	Right A1
	65	−35	35	−2.32	40	Right A1
	60	−35	30	−2.31	40	Right A1
	55	−30	35	−2.31	40	Right A1
	55	−30	25	−2.31	40	Right A1
	50	−30	30	−2.31	40	Right A1
	60	−30	25	−2.30	40	Right A1
	65	−30	40	−2.30	40	Right A1
	65	−25	35	−2.30	2	Right S1
Gamma	65	−25	40	−3.52	2	Right S1
	65	−25	35	−3.48	2	Right S1
	65	−20	40	−3.47	1	Right S1
	65	−30	40	−3.46	40	Right A1
	65	−20	35	−3.44	1	Right S1
	60	−25	40	−3.44	3	Right S1
	65	−30	35	−3.43	40	Right A1
	60	−25	35	−3.42	2	Right S1
	60	−20	40	−3.40	4	Right M1

Alpha1, 8–10 Hz; beta, 21.5–30 Hz; gamma, 30.5–45 Hz; S1, primary sensory cortex; M1, primary motor cortex.

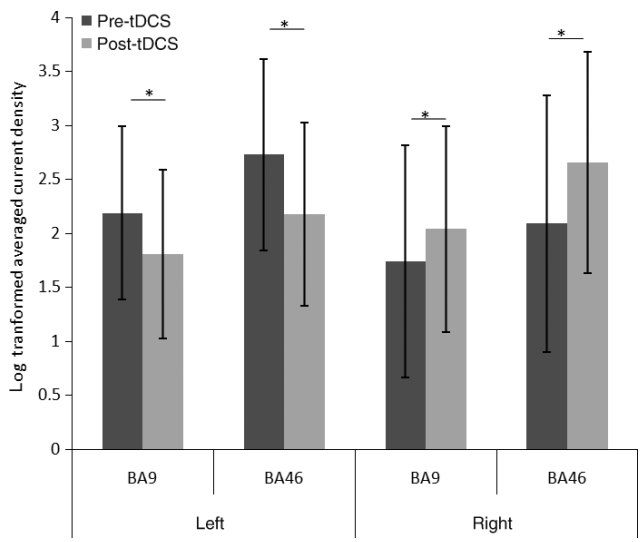

FIG. 3. Region of interest analysis for the left and right DLPFC pre-real and post-real tDCS for the gamma band frequency (*$P < 0.05$).

functional connectivity was also found between the left PHC and, respectively, the left DLPFC and the prACC. For the gamma frequency band, decreased functional connectivity was found between the right DLPFC and the left DLPFC, prACC, right A1 and left and right PHC comparing post-real tDCS with pre-real tDCS (see Fig. 4b). Decreased gamma functional connectivity was also found between the left DLPFC and the left PHC and prACC, and between the right A1 and the right PHC and the prACC.

Autocorrelation of the dorsolateral prefrontal cortex

Autocorrelations were very similar between the left and right DLPFC before tDCS, with high correlations between all frequencies within the 2–20 Hz range, and between all frequencies within the 20–45 Hz range (see Fig. 5). Correlations higher than 0.40 or lower than −0.40 were significant ($P < 0.05$).

In comparison to pre-tDCS, post-tDCS correlations between current densities for 2–20 Hz were decreased, for both the left and right DLPFC. High-frequency current density correlations were less attenuated.

Cross-correlation between the dorsolateral prefrontal cortex and, respectively, the pregenual anterior cingulate cortex, left parahippocampus, right parahippocampus and right primary auditory cortex

Before tDCS, the right and left PHC and A1 demonstrated very similar correlated activity with the right DLPFC, except for less correlated activity between low frequencies (2–10 Hz) of the DLPFC and high frequencies (30–45 Hz) of A1 (see Fig. 6). Correlations higher than 0.40 or lower than −0.40 were significant ($P < 0.05$). Correlated activity between the right DLPFC and prACC was almost an autocorrelation except for less correlated activity between low frequencies (2–10 Hz) of the DLPFC and high frequencies (30–45 Hz) of prACC. There was highly correlated activity between the beta band of the DLPFC and low gamma band activity of the prACC.

Bifrontal tDCS seemed to only exert minimal changes in the low-frequency correlated activity between the DLPFC and PrACC, but a theta (DLPFC) and beta (PrACC) disengagement post-real tDCS in comparison to pre-real tDCS was also noted.

The most striking finding, however, between pre- and post-tDCS was the similarity between the effect exerted by DLPFC tDCS on the right PHC and right A1 current densities, and the difference between the effect on the left and right PHC. More specifically, for the right PHC and right A1, only delta correlations and gamma correlated activity remained, with some beta–gamma correlated activity. For the PHC, bifrontal tDCS had a more pronounced impact on the left PHC in comparison to the right PHC. Post-tDCS, almost all activity between the DLPFC and left PHC became decorrelated, mostly between theta activity in the DLPFC and all activity in the left PHC. This same pattern of DLPFC theta decorrelation was noted to all other frequencies in the prACC, right PHC and right A1.

Comparing post-real tDCS with pre-real tDCS, a general trend was visible with decorrelated current density activity between theta for one region (respectively, prAAC, left and right PHC, and right A1 with right DLPFC and vice versa) and the higher frequency bands (respectively, prAAC, left and right PHC, and right A1 with right DLPFC and vice versa).

Pre- vs. post-sham transcranial direct current stimulation electroencephalography source analysis

The EEG source analysis revealed no significant effect post-sham tDCS in comparison to pre-sham tDCS for delta, theta, alpha1, alpha2, beta1, beta2, beta3 and gamma.

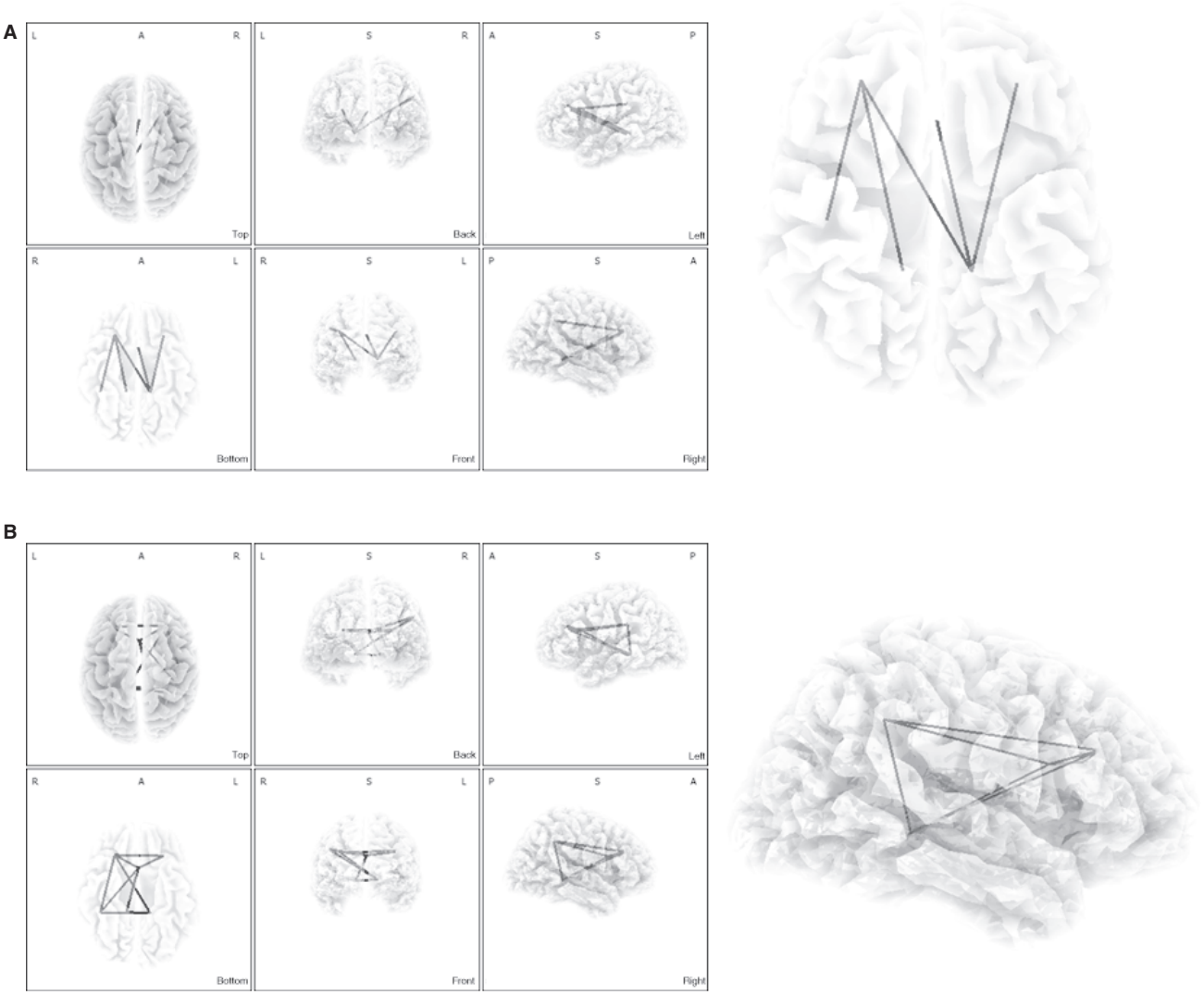

FIG. 4. Functional connectivity for the theta (A) and gamma (B) frequency bands when comparing pre-real and post-real tDCS. The red color shows increased connectivity, whereas the blue color shows decreased activity. A, anterior; L, left; P, posterior; R, right; S, superior. For interpretation of color references in figure legend, please refer to the Web version of this article.

Discussion

In the present work we demonstrated that, when electrodes are placed over the DLPFC (the anodal electrode overlying the right and the cathodal electrode overlying the left DLPFC), suppression of tinnitus intensity and tinnitus-related distress can be obtained associated with changes in spontaneous regional brain activity. More precisely, we found increased activity in the prACC for the alpha1 frequency band and decreased activity in the right A1 for the beta3 and gamma frequency band after real tDCS in comparison to pre-treatment. Furthermore, a region of interest analysis revealed for gamma activity an increase in the right DLPFC and a decrease in the left DLPFC after real tDCS. A comparison between pre- and post-sham tDCS revealed no significant differences in brain activity, suggesting that sham stimulation exerted no effect on brain activity.

In addition, connectivity analysis revealed a general decrease in gamma functional connectivity between the DLPFC, prACC, left and right PHC, and the right A1 when comparing post-real tDCS with pre-real tDCS. An opposite trend was found for theta connectivity, i.e. a general increase in functional theta connectivity between the DLPFC, prACC, left and right PHC, and the right A1 when comparing post-real tDCS with pre-real tDCS.

Autocorrelations for, respectively, the left and right DLPFC further revealed a decorrelation for low-frequency interspectral current density activity post-real tDCS in comparison to pre-real tDCS. Cross-correlations revealed disengagement between theta and, respectively, alpha and beta for the right DLPFC and, respectively, the prACC, left and right PHC and the right A1, and vice versa.

Pregenual anterior cingulate cortex, dorsolateral prefrontal cortex

Our results indicate that the spontaneous activity changes not only in the DLPFC but also in other brain areas such as the prACC and right A1. This is in accordance with a recent bifrontal tDCS study that revealed differences in current densities directly under the electrodes as well as in other brain structures (Sadleir *et al.*, 2010) functionally and topologically connected to the stimulated area (Polania *et al.*,

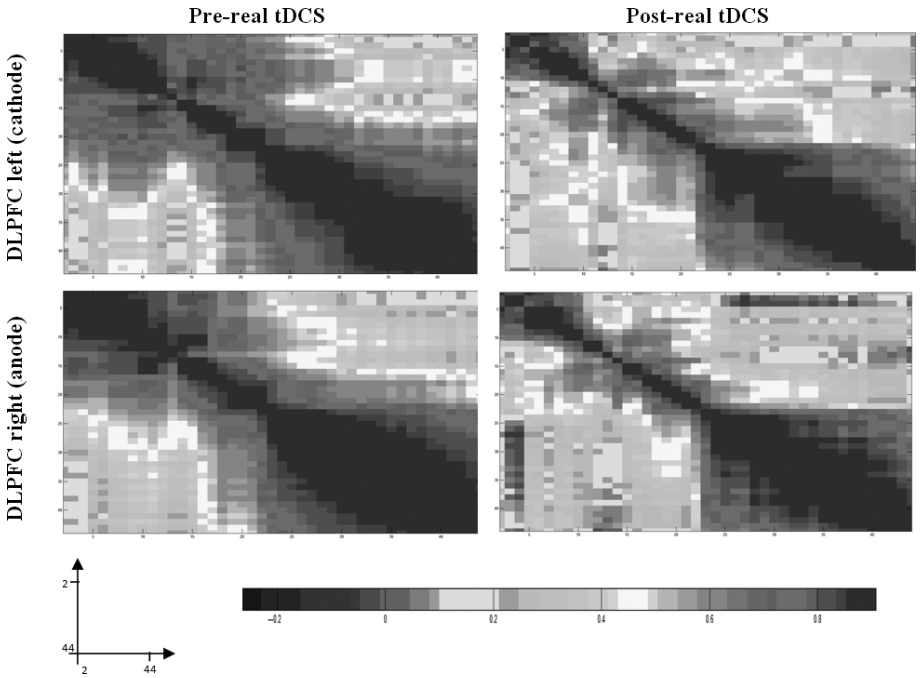

FIG. 5. Autocorrelations for log-transformed current density in the left and right DLPFC from 2 to 44 Hz ($r > 0.40$ is significant, $P < 0.05$).

2011). The DLPFC has reciprocal anatomical connections to the prACC (Pandya *et al.*, 1981; Vogt & Pandya, 1987; Yukie & Shibata, 2009), which has anatomical connections to the posterior parahippocampal area (Yukie & Shibata, 2009) and auditory cortex (Yukie & Shibata, 2009), permitting lagged phase functional connectivity changes within these areas.

Our results are in accordance with a previous study revealing that cathodal tDCS significantly decreased, whereas anodal tDCS slightly increased gamma frequency powers (Antal *et al.*, 2004). In addition, autocorrelations further demonstrated a desynchronization for inter-spectral current density correlations and disengagement between the frequency bands post-tDCS in comparison to pre-tDCS for the left and right DLPFC. The modulation of gamma oscillatory activity in the DLPFC has been closely related to several cognitive and behavioral processes (Farzan *et al.*, 2010).

After bifrontal tDCS, increased alpha activity was found in the prACC. Increased alpha activity has been found to correlate with reduced levels of anxiety (Cahn & Polich, 2006). The prACC has been implicated as the affective subdivision of the anterior cingulate cortex and a key target for antidepressant drugs (Bush *et al.*, 2000; Freedman *et al.*, 2000; Barbas *et al.*, 2003). This area is an important component of a network for mood regulation and related functions (Mayberg, 1997; Bush *et al.*, 2000; Freedman *et al.*, 2000; Barbas *et al.*, 2003). The prACC is a key marker of therapeutic response in depression treatment, including pharmacotherapy (Mayberg, 1997; Mulert *et al.*, 2007) and deep brain stimulation (Mayberg *et al.*, 2005). Its activity also predicts the amount of tinnitus distress reduction with transcranial magnetic stimulation targeting the superior temporal gyrus (Plewnia *et al.*, 2006). It has been shown that frontal lobotomies, which undercut the connections to the prefrontal cortex, do not seem to change the tinnitus intensity but rather the emotional (distress) component of the tinnitus (Elithorn, 1953; Beard, 1965). Therefore, modulating the frontal cortex by tDCS could influence the emotional component by similar mechanisms, albeit less invasive and less destructive.

Auditory cortex and parahippocampal cortex

Bilateral tDCS of the DLPFC might exert its tinnitus-suppressing effects via a combination of mechanisms, modulating both tinnitus intensity and tinnitus distress: tinnitus intensity by modulating gamma band activity in the auditory cortex (van der Loo *et al.*, 2009), and tinnitus distress by mediating an alpha-oscillation-controlled network consisting of the PHC, subgenual anterior cingulate cortex, amygdala and insula and associated beta activity in the dorsal anterior cingulate cortex (Vanneste *et al.*, 2010a). The DLPFC is connected with the ipsilateral auditory cortex via the PHC (Grunwald *et al.*, 2003; Boutros *et al.*, 2005, 2008; Korzyukov *et al.*, 2007), and the PHC is involved in sensory gating (Boutros *et al.*, 2008), i.e. reducing redundant or irrelevant auditory input.

Both animal and human invasive electrophysiological recordings in the PHC and hippocampus demonstrated that auditory sensory gating is mediated by a network, which includes the auditory cortex, cingulate cortex, prefrontal cortex and PHC (Grunwald *et al.*, 2003; Boutros *et al.*, 2005, 2008; Korzyukov *et al.*, 2007). Our connectivity results demonstrate that the gamma connectivity between the right DLPFC, PHC and auditory cortex decreased, whereas theta connectivity between these areas increased after tDCS. It is therefore possible that bifrontal tDCS induces parahippocampal sensory gating, and thereby modulates auditory cortex activity. A recent study demonstrated that tinnitus intensity is related to gamma band activity in the contralateral auditory cortex (van der Loo *et al.*, 2009). As bifrontal tDCS can suppress beta3 and gamma activity in A1, tDCS might have a direct or indirect effect on the tinnitus intensity. If unilateral tinnitus indeed originates from the contralateral auditory cortex gamma band activity, it is expected that tDCS with right anodal and left cathodal

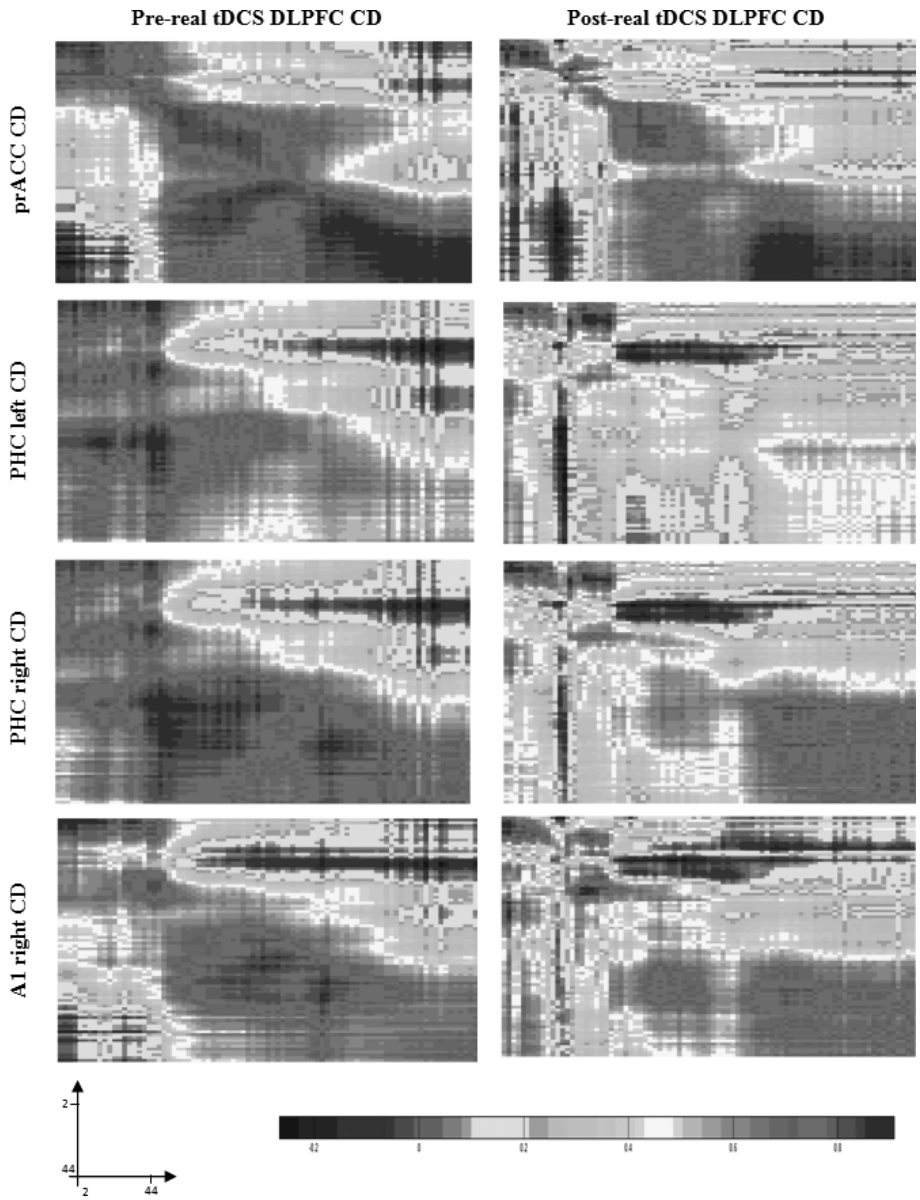

FIG. 6. Correlations for the log-transformed current density between the right DLPFC and, respectively, the prACC, left PHC, right PHC and A1 from 2 to 44 Hz. Left column demonstrates the current density (CD) correlations between the right DLPFC and PrACC, right DLPFC and left PHC, right DLPFC and right PHC, and right DLPFC and right A1. Right column demonstrates the CD correlations between the right DLPFC and PrACC, left and right PHC, and right A1 after anodal tDCS over the right DLPFC ($r > 0.40$ is significant, $P < 0.05$).

DLPFC stimulation would better suppress left-sided than right-sided tinnitus. This hypothesis was indeed confirmed in a previous bifrontal tDCS with the same stimulation protocol (Vanneste *et al.*, 2010a).

Autocorrelations and cross-correlations

As bifrontal tDCS decorrelates activity in the DLPFC and between the ACC, PHC, A1 and DLPFC between theta and alpha and beta might influence long-range connectivity. tDCS induces a lagged phase desynchronization of gamma band activity and increased lagged phase synchronization of the theta band. It is conceivable that bifrontal tDCS induces a cross-frequency decoupling between the DLPFC, PHC and A1. It has been shown that cross-frequency coupling of beta/gamma to theta phase is important for working memory (Axmacher *et al.*, 2010) and bifrontal tDCS can modulate working memory (Fregni *et al.*, 2005; Boggio *et al.*, 2006). Studies in the visual field further revealed that both perceived and non-perceived visual stimuli cause a similar increase of gamma oscillations in the EEG, but only perceived stimuli induce a transient long-distance synchronization of gamma oscillations across widely separated regions of the brain (Melloni *et al.*, 2007; Gaillard *et al.*, 2009). In addition, only visual stimuli that are consciously perceived induce enhanced theta oscillations over frontal regions and demonstrate an increase of the P300 component of the event-related potential, and an increase in power and phase synchrony of gamma oscillations (Melloni *et al.*, 2007). The question arises whether an analogous mechanism might occur in the auditory system. The P300 seems to interrupt and reset ongoing activity to what is being processed in the DLPFC, or in working memory (Manes *et al.*, 2002). It is therefore hypothetically conceivable that bifrontal tDCS modulates the tinnitus percept by cross-frequency decoupling in

the theta–beta/gamma network. However, further research is needed to confirm or disprove this hypothesis.

Conclusion

In conclusion, the present EEG study provides support that bifrontal tDCS with the anodal electrode overlying the right DLPFC and the cathodal electrode overlying the left DLPFC can suppress tinnitus intensity and tinnitus-related distress transiently. Bifrontal tDCS modulates the prACC, PHC areas and right A1 in resting-state spontaneous neuronal activity. These findings provide direct support that tDCS has an impact not only directly on the underlying DLPFC but also indirectly on other brain areas relevant for, respectively, tinnitus distress and tinnitus intensity.

Acknowledgement

The authors thank Jan Ost, Pieter Van Looy, Bram Van Achteren and Bjorn De Vree for their help in preparing this manuscript.

Abbreviations

A1, primary auditory cortex; BA, Brodmann area; DLPFC, dorsolateral prefrontal cortex; EEG, electroencephalography; ICA, independent component analysis; PHC, parahippocampus; prACC, pregenual anterior cingulate cortex; sLORETA, standardized low-resolution brain electromagnetic tomography; tDCS, transcranial direct current stimulation.

References

Antal, A., Kincses, T.Z., Nitsche, M.A., Bartfai, O. & Paulus, W. (2004) Excitability changes induced in the human primary visual cortex by transcranial direct current stimulation: direct electrophysiological evidence. *Invest. Ophthalmol. Vis. Sci.*, **45**, 702–707.

Axelsson, A. & Ringdahl, A. (1989) Tinnitus – a study of its prevalence and characteristics. *Br. J. Audiol.*, **23**, 53–62.

Axmacher, N., Henseler, M.M., Jensen, O., Weinreich, I., Elger, C.E. & Fell, J. (2010) Cross-frequency coupling supports multi-item working memory in the human hippocampus. *Proc. Natl. Acad. Sci. USA*, **107**, 3228–3233.

Barbas, H., Saha, S., Rempel-Clower, N. & Ghashghaei, T. (2003) Serial pathways from primate prefrontal cortex to autonomic areas may influence emotional expression. *BMC Neurosci.*, **4**, 25.

Beard, A.W. (1965) Results of leucotomy operations for tinnitus. *J. Psychosom. Res.*, **9**, 29–32.

Beeli, G., Casutt, G., Baumgartner, T. & Jancke, L. (2008) Modulating presence and impulsiveness by external stimulation of the brain. *Behav. Brain Funct.*, **4**, 33.

Boggio, P.S., Ferrucci, R., Rigonatti, S.P., Covre, P., Nitsche, M., Pascual-Leone, A. & Fregni, F. (2006) Effects of transcranial direct current stimulation on working memory in patients with Parkinson's disease. *J. Neurol. Sci.*, **249**, 31–38.

Boggio, P.S., Zaghi, S. & Fregni, F. (2009) Modulation of emotions associated with images of human pain using anodal transcranial direct current stimulation (tDCS). *Neuropsychologia*, **47**, 212–217.

Boutros, N.N., Trautner, P., Rosburg, T., Korzyukov, O., Grunwald, T., Schaller, C., Elger, C.E. & Kurthen, M. (2005) Sensory gating in the human hippocampal and rhinal regions. *Clin. Neurophysiol.*, **116**, 1967–1974.

Boutros, N.N., Mears, R., Pflieger, M.E., Moxon, K.A., Ludowig, E. & Rosburg, T. (2008) Sensory gating in the human hippocampal and rhinal regions: regional differences. *Hippocampus*, **18**, 310–316.

Bush, G., Luu, P. & Posner, M.I. (2000) Cognitive and emotional influences in anterior cingulate cortex. *Trends Cogn. Sci.*, **4**, 215–222.

Cahn, B.R. & Polich, J. (2006) Meditation states and traits: EEG, ERP, and neuroimaging studies. *Psychol. Bull.*, **132**, 180–211.

Congedo, M. (2002) *EureKa! (Version 3.0)* [Computer Software]. NovaTech EEG Inc, Knoxville, TN. Freeware available online: http://www.NovaTechEEG.

Cronlein, T., Langguth, B., Geisler, P. & Hajak, G. (2007) Tinnitus and insomnia. *Prog. Brain Res.*, **166**, 227–233.

Dierks, T., Jelic, V., Pascual-Marqui, R.D., Wahlund, L., Julin, P., Linden, D.E., Maurer, K., Winblad, B. & Nordberg, A. (2000) Spatial pattern of cerebral glucose metabolism (PET) correlates with localization of intracerebral EEG-generators in Alzheimer's disease. *Clin. Neurophysiol.*, **111**, 1817–1824.

Dymond, A.M., Coger, R.W. & Serafetinides, E.A. (1975) Intracerebral current levels in man during electrosleep therapy. *Biol. Psychiatry*, **10**, 101–104.

Elithorn, A. (1953) Prefrontal leucotomy in the treatment of tinnitus. *Proc. R. Soc. Med.*, **46**, 832–833.

Farzan, F., Barr, M.S., Levinson, A.J., Chen, R., Wong, W., Fitzgerald, P.B. & Daskalakis, Z.J. (2010) Evidence for gamma inhibition deficits in the dorsolateral prefrontal cortex of patients with schizophrenia. *Brain*, **133**, 1505–1544.

Freedman, L.J., Insel, T.R. & Smith, Y. (2000) Subcortical projections of area 25 (subgenual cortex) of the macaque monkey. *J. Comp. Neurol.*, **421**, 172–188.

Fregni, F., Boggio, P.S., Nitsche, M., Bermpohl, F., Antal, A., Feredoes, E., Marcolin, M.A., Rigonatti, S.P., Silva, M.T., Paulus, W. & Pascual-Leone, A. (2005) Anodal transcranial direct current stimulation of prefrontal cortex enhances working memory. *Exp. Brain Res.*, **166**, 23–30.

Fregni, F., Boggio, P.S., Nitsche, M.A., Marcolin, M.A., Rigonatti, S.P. & Pascual-Leone, A. (2006a) Treatment of major depression with transcranial direct current stimulation. *Bipolar Disord.*, **8**, 203–204.

Fregni, F., Marcondes, R., Boggio, P.S., Marcolin, M.A., Rigonatti, S.P., Sanchez, T.G., Nitsche, M.A. & Pascual-Leone, A. (2006b) Transient tinnitus suppression induced by repetitive transcranial magnetic stimulation and transcranial direct current stimulation. *Eur. J. Neurol.*, **13**, 996–1001.

Friston, K.J. (2005) Models of brain function in neuroimaging. *Annu. Rev. Psychol.*, **56**, 57–87.

Fuchs, M., Kastner, J., Wagner, M., Hawes, S. & Ebersole, J.S. (2002) A standardized boundary element method volume conductor model. *Clin. Neurophysiol.*, **113**, 702–712.

Gaillard, R., Dehaene, S., Adam, C., Clemenceau, S., Hasboun, D., Baulac, M., Cohen, L. & Naccache, L. (2009) Converging intracranial markers of conscious access. *PLoS Biol.*, **7**, e61.

Grunwald, T., Boutros, N.N., Pezer, N., von Oertzen, J., Fernandez, G., Schaller, C. & Elger, C.E. (2003) Neuronal substrates of sensory gating within the human brain. *Biol. Psychiatry*, **53**, 511–519.

Honey, C.J., Kotter, R., Breakspear, M. & Sporns, O. (2007) Network structure of cerebral cortex shapes functional connectivity on multiple time scales. *Proc. Natl. Acad. Sci. USA*, **104**, 10240–10245.

Jurcak, V., Tsuzuki, D. & Dan, I. (2007) 10/20, 10/10, and 10/5 systems revisited: their validity as relative head-surface-based positioning systems. *Neuroimage*, **34**, 1600–1611.

Knight, R.T., Scabini, D. & Woods, D.L. (1989) Prefrontal cortex gating of auditory transmission in humans. *Brain Res.*, **504**, 338–342.

Korzyukov, O., Pflieger, M.E., Wagner, M., Bowyer, S.M., Rosburg, T., Sundaresan, K., Elger, C.E. & Boutros, N.N. (2007) Generators of the intracranial P50 response in auditory sensory gating. *Neuroimage*, **35**, 814–826.

Langguth, B., Kleinjung, T., Fischer, B., Hajak, G., Eichhammer, P. & Sand, P.G. (2007) Tinnitus severity, depression, and the big five personality traits. *Prog. Brain Res.*, **166**, 221–225.

van der Loo, E., Gais, S., Congedo, M., Vanneste, S., Plazier, M., Menovsky, T., Van de Heyning, P. & De Ridder, D. (2009) Tinnitus intensity dependent gamma oscillations of the contralateral auditory cortex. *PLoS One*, **4**, e7396.

Manes, F., Sahakian, B., Clark, L., Rogers, R., Antoun, N., Aitken, M. & Robbins, T. (2002) Decision-making processes following damage to the prefrontal cortex. *Brain*, **125**, 624–639.

Mayberg, H.S. (1997) Limbic-cortical dysregulation: a proposed model of depression. *J. Neuropsychiatry Clin. Neurosci.*, **9**, 471–481.

Mayberg, H.S., Lozano, A.M., Voon, V., McNeely, H.E., Seminowicz, D., Hamani, C., Schwalb, J.M. & Kennedy, S.H. (2005) Deep brain stimulation for treatment-resistant depression. *Neuron*, **45**, 651–660.

Melloni, L., Molina, C., Pena, M., Torres, D., Singer, W. & Rodriguez, E. (2007) Synchronization of neural activity across cortical areas correlates with conscious perception. *J. Neurosci.*, **27**, 2858–2865.

Mulert, C., Jager, L., Schmitt, R., Bussfeld, P., Pogarell, O., Moller, H.J., Juckel, G. & Hegerl, U. (2004) Integration of fMRI and simultaneous EEG: towards a comprehensive understanding of localization and time-course of brain activity in target detection. *Neuroimage*, **22**, 83–94.

Mulert, C., Juckel, G., Brunnmeier, M., Karch, S., Leicht, G., Mergl, R., Moller, H.J., Hegerl, U. & Pogarell, O. (2007) Rostral anterior cingulate

cortex activity in the theta band predicts response to antidepressive medication. *Clin. EEG Neurosci.*, **38**, 78–81.
Nichols, T.E. & Holmes, A.P. (2002) Nonparametric permutation tests for functional neuroimaging: a primer with examples. *Hum. Brain Mapp.*, **15**, 1–25.
Nitsche, M.A. & Paulus, W. (2000) Excitability changes induced in the human motor cortex by weak transcranial direct current stimulation. *J. Physiol.*, **527**, 633–639.
Nitsche, M.A. & Paulus, W. (2001) Sustained excitability elevations induced by transcranial DC motor cortex stimulation in humans. *Neurology*, **57**, 1899–1901.
Nitsche, A., Muller, C.W., Radonic, A., Landt, O., Ellerbrok, H., Pauli, G. & Siegert, W. (2001) Human herpesvirus 6A DNA Is detected frequently in plasma but rarely in peripheral blood leukocytes of patients after bone marrow transplantation. *J. Infect. Dis.*, **183**, 130–133.
Nitsche, M.A., Liebetanz, D., Antal, A., Lang, N., Tergau, F. & Paulus, W. (2003) Modulation of cortical excitability by weak direct current stimulation–technical, safety and functional aspects. *Suppl. Clin. Neurophysiol.*, **56**, 255–276.
Pandya, D.N., Van Hoesen, G.W. & Mesulam, M.M. (1981) Efferent connections of the cingulate gyrus in the rhesus monkey. *Exp. Brain Res.*, **42**, 319–330.
Pascual-Marqui, R.D. (2002) Standardized low-resolution brain electromagnetic tomography (sLORETA): technical details. *Methods Find. Exp. Clin. Pharmacol.*, **24**(Suppl D), 5–12.
Pascual-Marqui, R. (2007a) Discrete, 3D distributed, linear imaging methods of electric neuronal activity. Part 1: exact, zero error localization. Available online at: http://arxiv.org/abs/0710.3341.
Pascual-Marqui, R. (2007b) Instantaneous and lagged measurements of linear and nonlinear dependence between groups of multivariate time series: frequency decomposition. Available online at: http://arxiv.org/abs/0711.1455.
Pizzagalli, D., Pascual-Marqui, R.D., Nitschke, J.B., Oakes, T.R., Larson, C.L., Abercrombie, H.C., Schaefer, S.M., Koger, J.V., Benca, R.M. & Davidson, R.J. (2001) Anterior cingulate activity as a predictor of degree of treatment response in major depression: evidence from brain electrical tomography analysis. *Am. J. Psychiatry*, **158**, 405–415.
Pizzagalli, D.A., Oakes, T.R., Fox, A.S., Chung, M.K., Larson, C.L., Abercrombie, H.C., Schaefer, S.M., Benca, R.M. & Davidson, R.J. (2004) Functional but not structural subgenual prefrontal cortex abnormalities in melancholia. *Mol. Psychiatry*, **9**, 325.
Plewnia, C., Reimold, M., Najib, A., Reischl, G., Plontke, S.K. & Gerloff, C. (2006) Moderate therapeutic efficacy of PET-navigated repetitive transcranial magnetic stimulation against chronic tinnitus: a randomised, controlled pilot study. *J. Neurol. Neurosurg. Psychiatry*, **78**, 152–156.
Polania, R., Nitsche, M.A. & Paulus, W. (2011) Modulating functional connectivity patterns and topological functional organization of the human brain with transcranial direct current stimulation. *Hum. Brain Mapp.*, **32**, 1236–1249.
Sadleir, R.J., Vannorsdall, T.D., Schretlen, D.J. & Gordon, B. (2010) Transcranial direct current stimulation (tDCS) in a realistic head model. *Neuroimage*, **51**, 1310–1318.
Schlee, W., Mueller, N., Hartmann, T., Keil, J., Lorenz, I. & Weisz, N. (2009) Mapping cortical hubs in tinnitus. *BMC Biol.*, **7**, 80.
Scott, B. & Lindberg, P. (2000) Psychological profile and somatic complaints between help-seeking and non-help-seeking tinnitus subjects. *Psychosomatics*, **41**, 347–352.
Sporns, O. & Kotter, R. (2004) Motifs in brain networks. *PLoS Biol.*, **2**, e369.
Sporns, O., Chialvo, D.R., Kaiser, M. & Hilgetag, C.C. (2004) Organization, development and function of complex brain networks. *Trends Cogn. Sci.*, **8**, 418–425.
Vanneste, S. & De Ridder, D. (eds) (2011) *A New Tool for the Treatment of Tinnitus*. Springer, New York.
Vanneste, S., Plazier, M., der Loo, E., de Heyning, P.V., Congedo, M. & De Ridder, D. (2010a) The neural correlates of tinnitus-related distress. *Neuroimage*, **52**, 470–480.
Vanneste, S., Plazier, M., Ost, J., van der Loo, E., Van de Heyning, P. & De Ridder, D. (2010b) Bilateral dorsolateral prefrontal cortex modulation for tinnitus by transcranial direct current stimulation: a preliminary clinical study. *Exp. Brain Res.*, **202**, 779–785.
Vanneste, S., Plazier, M., van der Loo, E., Van de Heyning, P. & De Ridder, D. (2010c) The differences in brain activity between narrow band noise and pure tone tinnitus. *PLoS One*, **5**, e13618.
Vanneste, S., Plazier, M., van der Loo, E., Van de Heyning, P. & De Ridder, D. (2011) The difference between uni- and bilateral auditory phantom percept. *Clin. Neurophysiol.*, **122**, 578–587.
Vitacco, D., Brandeis, D., Pascual-Marqui, R. & Martin, E. (2002) Correspondence of event-related potential tomography and functional magnetic resonance imaging during language processing. *Hum. Brain Mapp.*, **17**, 4–12.
Vogt, B.A. & Pandya, D.N. (1987) Cingulate cortex of the rhesus monkey: II. Cortical afferents. *J. Comp. Neurol.*, **262**, 271–289.
Volpe, U., Mucci, A., Bucci, P., Merlotti, E., Galderisi, S. & Maj, M. (2007) The cortical generators of P3a and P3b: a LORETA study. *Brain Res. Bull.*, **73**, 220–230.
Weisz, N., Muller, S., Schlee, W., Dohrmann, K., Hartmann, T. & Elbert, T. (2007) The neural code of auditory phantom perception. *J. Neurosci.*, **27**, 1479–1484.
Worrell, G.A., Lagerlund, T.D., Sharbrough, F.W., Brinkmann, B.H., Busacker, N.E., Cicora, K.M. & O'Brien, T.J. (2000) Localization of the epileptic focus by low-resolution electromagnetic tomography in patients with a lesion demonstrated by MRI. *Brain Topogr.*, **12**, 273–282.
Yukie, M. & Shibata, H. (2009) Temporocingulate Interactions in the Monkey. In Vogt, B. (Ed.), *Cingulate Neurobiology and Disease*. Oxford University Press, Oxford, pp. 145–162.
Zumsteg, D., Wennberg, R.A., Treyer, V., Buck, A. & Wieser, H.G. (2005) H2(15)O or 13NH3 PET and electromagnetic tomography (LORETA) during partial status epilepticus. *Neurology*, **65**, 1657–1660.
Zumsteg, D., Lozano, A.M. & Wennberg, R.A. (2006a) Depth electrode recorded cerebral responses with deep brain stimulation of the anterior thalamus for epilepsy. *Clin. Neurophysiol.*, **117**, 1602–1609.
Zumsteg, D., Lozano, A.M. & Wennberg, R.A. (2006b) Mesial temporal inhibition in a patient with deep brain stimulation of the anterior thalamus for epilepsy. *Epilepsia*, **47**, 1958–1962.
Zumsteg, D., Lozano, A.M., Wieser, H.G. & Wennberg, R.A. (2006c) Cortical activation with deep brain stimulation of the anterior thalamus for epilepsy. *Clin. Neurophysiol.*, **117**, 192–207.